J. Iran. Chem. Soc., Vol. 6, No. 2, June 2009, pp. 230-242.

JOURNAL OF THE
Iranian
Chemical Society

The Heat of Vaporization and Nanocavity Formation

K. Azizi[a] and A. Nasehzadeh[b,]*
[a]*Department of Chemistry, Faculty of Science, University of Kurdistan, Sanandaj, 66177, Iran*
[b]*Department of Chemistry, Shahid Bahonar University, Kerman 76175, Iran*

(Received 28 December 2007, Accepted 2 April 2008)

Two distinct approaches are used to derive a unique and exact analytical expression for the heat of vaporization with respect to the nanocavity energy formation and the molecular hard-core diameter. This expression provides a new method to compare different models of cavity formation in the liquids as well as to predict the effective molecular hard-core diameter at different temperatures and pressures. The effective hard-core diameters and cavity formation energies of liquid Ar, Xe and CH_4 are calculated at various temperatures and pressures using different cavity formation models and they are compared. It is found that the effective hard-core diameter generally decreases with increase of temperature as expected and it increases with increase of pressure.

Keywords: Dense fluids, Nanocavity formation energy, Hard-core diameter, Heat of vaporization

INTRODUCTION

The energy of solvation is considered to be the result of the compensation between the positive cavity formation energy (CFE) and the negative stabilization energy of attractions [1] and, therefore, accurate calculation of each term is an important theoretical challenge. The CFE may be studied by using hard sphere (HS) models, which is the subject of the present study. It should be noted that if the CFE could be correctly predicted, then evaluation of the energy of attraction would be possible. Therefore, accurate prediction of cavity formation energy could be an important ingredient of thermodynamic perturbation and variational theories [2], which are based on the hard-sphere fluid properties and an interesting subject in the treatment of statistical thermodynamics of dense fluids [3-7].

The analytical expressions for the CFE of a hard sphere (HS) solute in a HS solvent are available from the Scaled-Particle Theory (SPT) [8] and Mansoori-Carnahan-Starling-Leland (MCSL) equation of state for HS mixtures [9]. The MCSL has been tested by the Widom test particle insertion method [10-12] for calculating the excess chemical potential of dissolved hard sphere solute in hard sphere solvent and was found to be an exact approach and superior to the SPT. However, the Widom test particle method is practically limited to the liquids of low densities and of small size of the probe particles [12,13]. Matyushov and Ladanyi (ML) [14] have also tested the MCSL in the range of high liquid densities and relatively large sizes of insertion probes *i.e.,* where the Widom test particle method can not be used to test the MCSL analytical expression of cavity formation energy and have introduced some modifications to it.

The effective hard-sphere diameter (EHSD) of a real fluid is an important parameter, which significantly affects the results of CFE models [15]. Different values of EHSD have been obtained by using various independent techniques [16-

*Corresponding author. E-mail: asadnasehzadeh@yahoo.com

17] and their application gives different results for CFE. Therefore, evaluation of CFE expressions would be ambiguous. Obviously the values of EHSD, which obtained by any method suites for its own technique, therefore it would be worthwhile to evaluate the CFE expression by using the EHSD values that obtained by corresponding technique.

Although the applicability of the CFE expressions has been studied, the validity of the thermodynamic properties, which can be obtained from the CFE expressions have not been investigated. Obviously the final judgment about the validity of any cavity formation model, which may result in an analytic expression for CFE, depends on the validity of the thermodynamic properties, which are originated from the CFE expression.

It should be noted that there is no experimental values available for CFE for real molecules. Computer simulation using Monte Carlo method has predicted the only reliable data for CFE but for model molecules only [11-13].

In this work, which is a complementary of our previous work [18], we present an analytical expression for the heat of vaporization (ΔH_{vap}), which originates from the CFE expression. The validity of different CFE models is then examined by using the experimental values of ΔH_{vap} instead of the predicted values of CFE. The ability of analytical expressions to predict the values of EHSD for any compound at any given pressure and temperature is also presented. Since the reliable experimental data are needed to test the method, therefore Ar, Xe as simple spherical molecules and CH_4 as a spherically symmetric molecule, for which sufficient desired thermodynamic data have been reported in the literature, are investigated here.

APPROACHES

Approach 1

Energy of solvation in liquids is considered to be the result of compensation between the positive repulsive CFE and the negative attractive stabilization energy. In dealing with hard sphere fluids the hard-sphere potential energy (ϕ_h) of interaction between molecules is represented [19] by:

$$\phi_h = \infty, \qquad r \le \sigma \tag{1}$$

$$\phi_h = 0, \qquad r > \sigma \tag{2}$$

where σ and r are the hard sphere diameter and the distance between the centers of two adjacent molecules, respectively. Furthermore, in addition to ϕ_h, real molecules have a non-rigid or attractive potential (ϕ_a). The whole potential (ϕ) then is:

$$\phi = \phi_h + \phi_a \tag{3}$$

Therefore, the chemical potential of fluid can be written [19] as:

$$\mu = \mu_h + \mu_a \tag{4}$$

where μ_h is the chemical potential of a hard sphere system and it has been defined as [20]:

$$\mu_h = kT \ln(\rho \Lambda^3 / q\ ) + W^l_{cav,\,h} \tag{5}$$

where ρ is the number density, $1/\rho\ \Lambda^3$ and q are the partition functions for the translational and internal degrees of freedom, $\Lambda = h/(2\pi m\ kT)^{1/2}$ is the thermal wave length, m is the molecular mass, h is the Planck's constant, k is the Boltzman constant, T is absolute temperature and $W^l_{cav,\,h}$ is the reversible work of creating a cavity in hard sphere fluid with suitable size to accommodate the solute molecule. Substitution of Eq. (4) by Eq. (5) will give the chemical potential of the liquid

$$\mu^l = kT \ln(\rho \Lambda^3 / q) + W^l_{cav,\,h} + \mu^l_a \tag{6}$$

and for a very diluted gas which is considered to behave ideal

$$\mu^{id-g} = kT \ln(p_0 \Lambda^3 / kTq) \tag{7}$$

where p_0 is the pressure at which the vapor has nearly ideal behavior. Subtracting Eq. (6) from Eq. (7) gives

$$\mu^{id-g} - \mu^l = kT \ln(p_0 / \rho kT) - W^l_{cav,\,h} - \mu^l_a \tag{8}$$

Based on the Scheme 1, the left hand side term can be given as

$$\mu^{id-g} - \mu^l = (\mu^l_{eq} - \mu^l) + (\mu^g_{eq} - \mu^l_{eq}) + (\mu^{id-g} - \mu^g_{eq}) \tag{9}$$

where μ^l_{eq} and μ^g_{eq} are chemical potentials of an equilibrium gas-

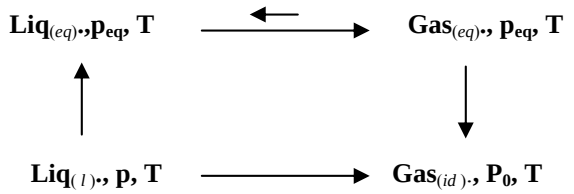

Scheme 1. Schematic of evaporation of a liquid at given temperature and pressure.

liquid system at temperature T and a given pressure p_{eq}. We may now simplify Eq. (9) into

$$\mu^{id-g} - \mu^{l} = (\mu^{g}_{eq} - \mu^{l}) + (\mu^{id-g} - \mu^{g}_{eq}) \tag{10}$$

Existing the reliable thermodynamic data allows the calculation of the first term on the right hand side of Eq. (10) and the second term is the change in chemical potential of a real gas when at a constant temperature its pressure decreases from p_{eq} to p_0.

Assuming that the equation of state of real gas is

$$pv_g = kT + \sum_{j=0}^{\infty} p^{(j+1)} B_{2+j} \tag{11}$$

where B_2, B_3, ... are the second, third, ... virial coefficients. Then, the second right hand term in Eq. (10) is given by:

$$\mu^{id-g} - \mu^{g}_{eq} = kT \ln(p_0 / p_{eq}) + \sum_{j=0}^{\infty} \frac{1}{j+1} B_{j+2} \left[p_0^{(j+1)} - p_{eq}^{(j+1)} \right] \tag{12}$$

Combination of Eqs. (8, 10) and (12) gives

$$\mu^{l}_{a} = kT \ln(p_0 / \rho kT) - W^{l}_{cav,h} - kT \ln(p_0 / p_{eq}) - \sum_{j=0}^{\infty} \frac{1}{j+1} B_{j+2} \left[p_0^{(j+1)} - p_{eq}^{(j+1)} \right] - (\mu^{g}_{eq} - \mu^{l}) \tag{13}$$

In general μ^{l}_{a} can also be decomposed as follows:

$$\mu^{l}_{a} = e^{l}_{a} + pv^{l}_{a} - Ts^{l}_{a} \tag{14}$$

where e^{l}_{a}, v^{l}_{a}, s^{l}_{a} are internal energy, volume and entropy, respectively, associated with the attractive potential. If the vapor is ideal, pv^{g} can be replaced by kT, then [21,22].

$$e^{l}_{a} = 2kT - 2pv^{l} - 2\lambda^{id}_{v} \tag{15}$$

where v^{l} is the liquid volume per molecule and λ^{id}_{v} is the heat of evaporation of the liquid into an ideal gas per molecule. If μ^{l}_{a} is known over a range of values of the state variables then s^{l}_{a} and v^{l}_{a} can be computed through the following thermodynamic relations.

$$s_a = -(\partial \mu_a / \partial T)_p \tag{16}$$

$$v_a = (\partial \mu_a / \partial p)_T \tag{17}$$

Combination of Eqs. (14-16) leads to

$$\lambda^{id}_{v} = kT - pv^{l} + \frac{1}{2}\left[pv^{l}_{a} - \mu^{l}_{a} + T(\partial \mu^{l}_{a} / \partial T)_p \right] \tag{18}$$

In order to derive an expression for $(\partial \mu^{l}_{a} / \partial T)_p$ using Eq. (13) we need to have an expression for $W^{h}_{cav,l}$ which appears in this equation. Various expressions can be obtained for $W^{h}_{cav,l}$ by using SPT, MCSL [8,9] or ML [14] models

$$W^{SPT}_{cav,l} = kT\left[-\ln(1-y) + 6\left[y/(1-y) \right] + \frac{9}{2}\left[y/(1-y) \right]^2 \right] + p\pi\sigma^3/6 \tag{19}$$

$$W^{MCSL}_{cav,l} = kT\left[3\left[y/(1-y) \right] + 3\left[y/(1-y)^2 \right] + 2\left[y/(1-y)^3 \right] \right] \tag{20}$$

$$W^{ML}_{cav,l} = kT\left[-\ln(1-y) + 3\left[y/(1-y) \right] + \left[\frac{3y(2-y)(1+y)}{2(1-y)^2} \right] + \left[\frac{y(1+y+y^2-y^3)}{(1-y)^3} \right] \right] \tag{21}$$

where $y = \pi\rho\sigma^3/6$ in which σ is the hard sphere diameter of molecules.

Using Eqs. (18-21) in (13) leads to the following expression:

$$\mu_a^l - T(\frac{\partial \mu_s^l}{\partial T})_p = kT - kT^2\alpha_p\eta^{cfm}(y) - p\vartheta^{cfm} - (\bar{h}_{eq}^g - \bar{h}^l) - \sum_{j=0}^{\infty}\frac{1}{j+1}(p_0^{(j+1)} - p_{eq}^{(j+1)})\left[B_{j+2} - T(\frac{\partial B_{j+2}}{\partial T})_p\right] \quad (22)$$

where superscript *cfm* is an abbreviation for *cavity formation models* such as $SPT, MCSL$ or ML, ϑ^{cfm} is a volume term which vanishes in the cases of MCSL and ML models and its value for SPT model is $\pi\sigma^3/6$, α_p is the coefficient of thermal expansion of liquid, $\bar{h}^i$ is the enthalpy of system i per molecule and $\eta^{cfm}(y)$ is some function of y which assume the following forms for different hard-sphere models

$$\eta^{SPT}(y) = \frac{(1+2y)^2}{(1-y)^3} \quad (23)$$

$$\eta^{MCSL}(y) = \frac{y^4 - 4y^3 + 4y^2 + 4y + 1}{(1-y)^4} \quad (24)$$

$$\eta^{ML}(y) = \frac{-y^5 + 4y^4 - 9y^3 + 8y^2 + 8y + 2}{2(1-y)^4} \quad (25)$$

Differentiating the both sides of Eq. (4) with respect to the pressure at constant temperature gives

$$v^l = v_a^l + v_h^l \quad (26)$$

The second term on the right hand side is in fact $(\partial\mu_h/\partial T)_p$, which can be calculated by using Eq. (5). Since Eq. (5) includes $W_{cav,h}^l$, therefore any of Eqs. (19-21) may be used, however the result can be given in a general form as

$$v_h^{l,cfm} = kT\beta_T\eta^{cfm}(y) + \vartheta^{cfm} \quad (27)$$

where β_T is the isothermal compressibility coefficient of liquid.

Combining Eqs. (18) and (22) and replacing from Eqs. (23-25) and (27) gives

$$\lambda_v^{id} = kT - \frac{1}{2}\Big[pv^l + kT - kT\eta^{cfm}(y)\left[T\alpha_p - p\beta_T\right] - (\bar{h}_{eq}^g - \bar{h}^l) - \sum_{j=0}^{\infty}\frac{1}{j+1}(p_0^{(j+1)} - p_{eq}^{(j+1)})\left[B_{j+2} - T(\frac{\partial B_{j+2}}{\partial T})_p\right]\Big] \quad (28)$$

Inserting Eq. (12) into Eq. (10) will gives

$$\mu^{id-g} - \mu^l = (\mu_{eq}^g - \mu^l) + kT\ln(p_0/p_{eq}) + \sum_{j=0}^{\infty}\frac{1}{j+1}B_{j+2}\left[p_0^{(j+1)} - p_{eq}^{(j+1)}\right] \quad (29)$$

Applying the Gibbs-Helmholtz relation on the both sides of Eq. (29) leads to

$$\bar{h}^{id-g} - \bar{h}^l = (\bar{h}_{eq}^g - \bar{h}^l) + \sum_{j=0}^{\infty}\frac{1}{j+1}(p_0^{(j+1)} - p_{eq}^{(j+1)})\left[B_{j+2} - T(\frac{\partial B_{j+2}}{\partial T})_p\right] \quad (30)$$

The left hand side term of Eq. (30) is in fact λ_v^{id}. Therefore, replacing the last two terms on the right hand side of Eq. (28) by λ_v^{id}, then rearranging and multiplying the result by Avogadro's number, N_A, gives

$$\Delta\bar{H}_{vap} = RT - p\bar{V}_l + RT\eta^{cfm}(y)\left[T\alpha_p - p\beta_T\right] \quad (31)$$

where $\bar{V}_l$ is the molar volume of the liquid and R is the gas constant. At formal pressures $p\bar{V}_l/RT << 1$ and $\beta_T p\eta^{cfm}(y) << 1$ which in turn simplifies Eq. (31) to

$$\Delta\bar{H}_{vap} = RT + RT^2\alpha_p\eta^{cfm}(y) \quad (32)$$

Approach 2

In this approach we start with the free energy of solution of a gaseous solute in a solvent which has been given [1] as

$$\Delta\bar{G}_{sol} = \bar{G}_c + \bar{G}_i + RT\ln(RT/\bar{V}_l) \quad (33)$$

where $\bar{G}_c$ and $\bar{G}_i$ are the molar free energy of cavity formation and solute-solvent interaction, respectively. Although Eq. (33) was initially introduced and applied for binary systems, it is also applicable for pure systems, *i.e.* the solute and the solvent are the same. In this case, for a pure system at a constant temperature and pressure, the solution and the evaporation process are exactly the inverse of one another, *i.e.*, $\Delta\bar{G}_{sol} = -\Delta\bar{G}_{vap}$ (for pure systems), hence

$$\Delta\bar{G}_{vap} = -\bar{G}_c - \bar{G}_i - RT\ln(RT/\bar{V}_l) \quad (34)$$

Applying the Gibbs-Helmholts relation on the both sides of Eq. (34) gives

$$\Delta\overline{H}_{vap} = -\overline{H}_c - \overline{H}_i + RT - \alpha_p RT^2 \tag{35}$$

In Eq. (34) $\overline{G}_c$ is in fact $W^h_{cav,l}$ multiplied by N_A, therefore any one of Eqs. (19-21) can be used to evaluate $\overline{H}_c = [\partial(\overline{G}_c/T)/\partial(1/T)]_p$. However a general form as may indicate the result is

$$\overline{H}_c^{cfm} = \alpha_p RT^2\left[\eta^{cfm}(y) - 1\right] + p\overline{\vartheta}^{cfm} \tag{36}$$

Using Eqs. (15) and (26), the value of $\overline{H}_i$ can be predicted

$$\overline{H}_i = 2RT - 2\Delta\overline{H}_{vap} - p(\overline{V}_l + \overline{V}_h^l) \tag{37}$$

Now an analytical expression for ΔH_{vap}, which is exactly the same as Eq. (34), is obtained by inserting (36) and (37) into Eq. (35) and using Eq. (27)

Considering that the above two distinct approaches have resulted in the same analytical expression for the heat of vaporization is a strong indication of the exactness of Eq. (31). In the following section we utilize Eq. (31) to evaluate the cavity formation energies and to calculate the hard-sphere diameters of various real molecules in liquid state using the heat of vaporization and other thermodynamic properties as appear in Eq. (31) with consideration of various hard-sphere equations of state.

RESULTS AND DISCUSSION

Since Eq. (31) is an exact consequence of the assumed form of CFE; therefore, it may directly be used to calculate the values of the effective hard-sphere diameter (σ_{eff}), which is the only adjustable parameter that affects the results of the CFE models. Therefore, the obtained values of σ_{eff} can then be used for evaluation and comparison of different CFE models.

Using Eq. (31) along with the experimental data of heat of vaporization, molar volume, α_p, and β_T of various substances one can predict the values of $\eta^l(y)$. Since $\eta^l(y)$ is a function of y, according to various models proposed above, one can calculate the effective hard-core diameter ($\sigma_{eff} = [6y/(\pi.\rho)]^{1/3}$) for various liquids at different temperatures and pressures. The values of physical properties such as ρ_l (density), $\Delta\overline{H}_f$ (molar enthalpy of formation for gas and liquid), $\overline{C}_p$ (molar heat capacity at constant pressure), $\overline{C}_v$ (molar heat capacity at constant volume), $C_\circ$ (speed of sound), which were needed in our calculations, were taken from Refs. [24-26]. The isothermal compressibility and the thermal expansion coefficients [23] needed in our calculations were calculated by:

$$\beta_T = \gamma_c / \rho_l c_0^2 \tag{38}$$

$$\alpha_p = \left[\frac{\gamma_c \overline{C}_V (\gamma_c - 1)}{MTc_0^2}\right]^{1/2} \tag{39}$$

where $\gamma_c = C_p/C_V$ is the ratio of heat capacities at constant pressure and constant volumes, ρ_l is the density of liquid, M is the molar mass, and c_0 is the speed of sound.

The values of σ_{eff} which were predicted at different temperatures and pressures along the coexistence liquid-gas line are given in Table 1. Application of these values into Eq. (21) will obviously give the values for cavity formation energy. Although there are no experimental values of CFE to be compared with, it has a singular value at any given temperature and pressure, which must be predicted by any model. Figure 1 which is typically plotted for Ar illustrates this argument. Figure 2 also shows the predicted values of CFE for Ar, Xe and CH_4. Figure 2 indicates while the values of $T \to T_c$, the values of $CFE \to 0$. This prediction is due to the application of unrealistic values of σ_{eff} which are obtained by Eq. (31) in this region.

The more direct approach for evaluation and comparison of different CFE models is to compare the values of heat of vaporization, which are predicted by Eq. (31) with experimental values.

Mayer [27] has used SPT to calculate the values of σ_{eff} for various substances at two different temperatures by using experimental data of surface tension and compressibility. We have repeated Mayer's method at more temperatures where reliable and desired experimental data of surface tension and compressibility are known [28]. Since the Mayer's compressibility approach consists of the Percus-Yevick

Table 1. Different Values of Effective Hard Spherical Diameters (Å) of Ar Predicted by Different Models Along the Vapour-Liquid Coexistence Line

	ΔH_{vap}			Mayer			
T (K)	SPT	MCSL	ML	Surf	PY*c*	PY*v*	CS
83.8	3.46233	3.30764	3.30888		3.23768	3.31648	3.25996
84	3.46021	3.30553	3.30677	3.18841	3.23554	3.31407	3.25776
85	3.45173	3.29707	3.29831	3.17762	3.22856	3.30607	3.25054
86	3.44259	3.28796	3.2892	3.16722	3.22064	3.29704	3.24237
87	3.43341	3.27881	3.28006	3.15672	3.21267	3.28796	3.23414
88	3.42453	3.26997	3.27122	3.14540	3.20542	3.27965	3.22664
89	3.41484	3.26036	3.26161	3.13451	3.19698	3.27006	3.21794
90	3.40533	3.25094	3.25218	3.12279	3.18869	3.26063	3.20936
91	3.39526	3.24098	3.24222		3.18002	3.25077	3.20041
92	3.38568	3.23152	3.23276		3.17209	3.24173	3.19222
93	3.37541	3.22137	3.22262		3.16328	3.23174	3.18312
94	3.36486	3.21098	3.21222		3.15405	3.22127	3.17358
95	3.35431	3.20061	3.20185		3.14482	3.21081	3.16405
96	3.34346	3.18995	3.19119		3.13546	3.20023	3.15439
97	3.33239	3.17909	3.18032		3.12582	3.18934	3.14443
98	3.32095	3.16789	3.16911		3.11577	3.17802	3.13406
99	3.30953	3.15672	3.15794		3.10583	3.16679	3.12378
102	3.27307	3.12114	3.12234		3.07409	3.13115	3.09105
105	3.23327	3.08246	3.08363		3.03880	3.09174	3.05466
108	3.18898	3.03959	3.04071		2.99879	3.04736	3.01347
111	3.14068	2.99299	2.99406		2.95513	2.99923	2.96858
114	3.08560	2.94004	2.94104		2.90479	2.94417	2.91691
117	3.02361	2.88062	2.88154		2.84862	2.88321	2.85937
120	2.95017	2.81044	2.81126		2.78040	2.80985	2.78964

SPT: Scaled Particle Theory, MCSL: Mansoori-Carnahan-Starling-Leland, ML: Matyushov-Ladanyi, Surf. = surface tension, PY*c*: Mayer's compressibility approach consists of the Percus-Yevick equation of state PY*v*:Percus-Yevik (virial approach), CS: Carnahan-Starling. Insignificant digits are retained to avoid round-off errors.

equation of state (compressibility approach, here after denoted as PYc), one may think of using the other equations of state of hard spherical systems. We have also derived the following compressibility equations by applying the Percus-Yevick equation of state (virial coefficients approach, here after denoted as PYv) and also Carnaham-Starling equation of state [29] (here after denoted as CS).

$$\beta_T^{PYv} = (\overline{V}_l / RT)[(1-y)^3/(1+5y+9y^2-3y^3)] \quad (40)$$

$$\beta_T^{CS} = (\overline{V}_l / RT)[(1-y)^3/(1+5y+9y^2-3y^3)] \quad (41)$$

These equations were also used to predict the values of σ_{eff}.

Typical results for Ar are shown in Table 1. The values of σ_{eff} which were predicted by using the Mayer's method (Table 1, columns 5-8) were taken as the results of independent techniques and used to predict the values of ΔH_{vap}, which in turn they were used for evaluation and comparison of three different CFE models, *i.e.*, SPT, MCSL

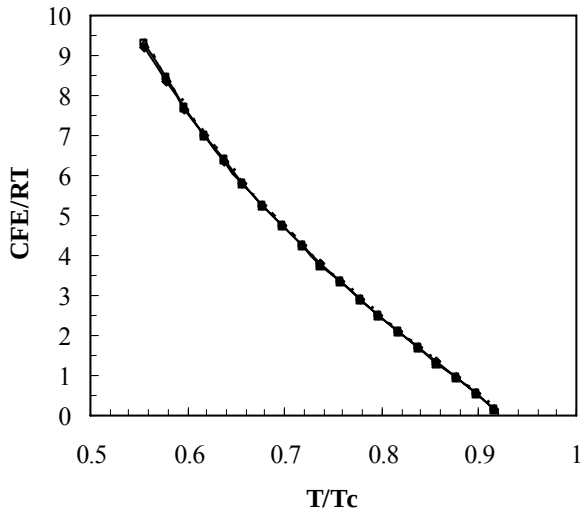

Fig. 1. Cavity formation energies of Ar predicted by using the values of EHSD obtained by Eq. (34).

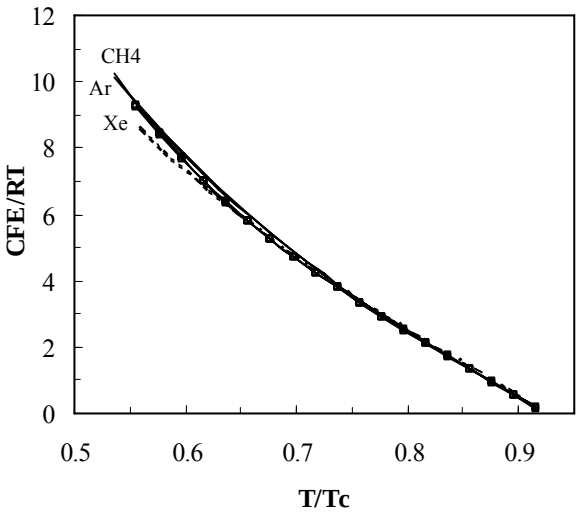

Fig. 2. Cavity formation energies of Ar, Xe and CH_4 predicted by using the values of EHSD obtained by Eq. (34).

and ML through Eq. (31). Therefore, there are 12 predicted values of ΔH_{vap} at each temperature, denoted as $\Delta H_{vap}^{cfm-mpd}$.

The general superscript *mpd* is an abbreviation for the Mayer's method of the prediction of the hard-sphere diameters and is classified as surface tension (denoted as *su*) and compressibility (denoted as *comp* which is substituted with PYcC, PYvC and CSC abbreviations depending on the type of applied equation of state) approaches. The experimental and

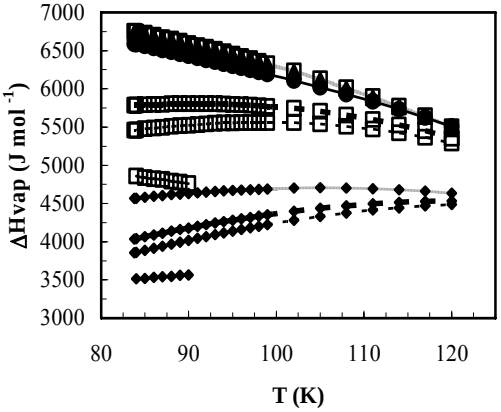

Fig. 3. A comparison between the experimental and predicted values of heat of vaporizations: (♦) SPT, (□) MCSL and (▲) ML, (●) ΔH_{vap}^{exp}, (—) su, (---) PYc, (···) PYv, (▪▪▪) CS.

predicted values of heat of vaporizations are compared in Fig. 3. It should be mentioned that, for any set of σ_{eff}, the predicted values of ΔH_{vap} through MCSL and ML models are nearly the same; therefore to avoid any complication, the predictions of ML method have not been presented, necessarily. This figure also indicates that:

1. The class of ΔH_{vap}^{cfm-su} has the worst agreement with the values of ΔH_{vap}^{exp}; therefore, the surface tension and its curvature dependence expressions [3] which were used by Mayer are inaccurate. Since this terms (the second and the third term in Eq. (19)) form the major portion of the CFE expression in the SPT, therefore it can be expected that the SPT model for CFE may include the inevitable deviations. The more remarkable point which is understood from the class of ΔH_{vap}^{cfm-su} is that, when the values of σ_{eff}, predicted by using the SPT through the Mayer's surface tension approach, applied into the three CFE models by using Eq. (31), the worse results are again correspond to the SPT predictions. Therefore, from the point of Eq. (31) view the MCSL and ML models are more accurate than SPT, even though the utilized values of σ_{eff} may bear some systematic errors.

2. The MCSL and ML models of CFE are more reasonable than SPT. This is in agreement with the predictions of Monte Carlo method [12] and also confirms the above discussion.

3. The accuracy of CS equation of state [29] in comparison

with the PYC, is also proved by Eq. (31).

4. The best and the worst values of σ_{eff} are those predicted by the PYvC approach and the surface tension approach, respectively. Therefore Eq. (31) can be used for evaluation and comparison of different methods for the prediction of effective hard-sphere diameters.

5. The values of $\Delta H_{vap}^{cfm-PYvC}$ indicate that, at low temperatures, the predictions of ML model is slightly better than the MCSL model. Therefore, Eq. (31) proves that the Matyushov and Ladanyi have exerted the proper modification on the MCSL model.

Figure 4 shows a comparison between the values of σ_{eff} listed in Table 1 and indicates that the values of σ_{eff} predicted by using the SPT model are larger than those predicted by using the other approaches, while the values of $\partial\sigma_{eff}/\partial T$ remains almost the same. This should be mentioned that surface tension and compressibility's expressions used by Mayer are originated from SPT as well as the heat of vaporization's expression. Therefore, one may expect to obtain the same values for HSD by using any of three expressions *i.e.,* surface tension, compressibility or heat of vaporization.

Here, we do not wish to explain discrepancy between surface tension and compressibility predictions, but we would like to discuss the origin of discrepancy in σ_{eff} values predicted either by surface tension or compressibility and heat of vaporizations to some extent. The surface tension or compressibility expressions used by Mayer are in fact applicable to hard spherical fluids and if applied to real fluids some deviations in results can be expected. While, both hard and soft potentials have been considered in derivation of analytical expression for heat of vaporization and considering the soft potential in turn helps to treat a fluid as close as to a real one. This can then be pretended that the results are obtained by Eq. (31) have more compatibility with reality. The values of σ_{eff} presented in Fig. 4 were predicted at both different temperatures and pressures along the liquid-gas coexistence line. We have also predicted the values of σ_{eff} for Ar and Xe and CH_4 at different temperatures and constant pressure and *vice versa*. An arbitrary constant pressure of 6.0 MPa was used to show that the proposed method could be applied at any desired pressure even at upper critical point

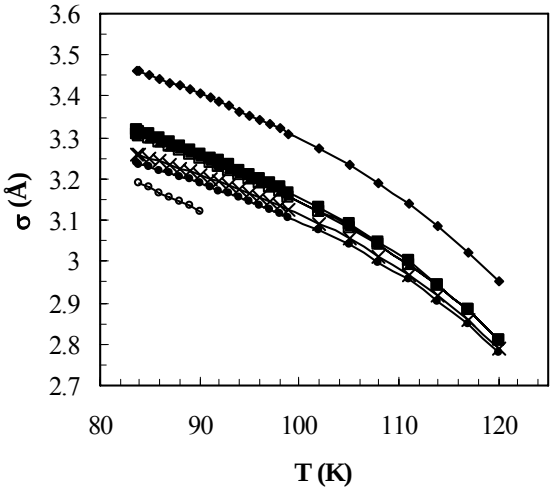

Fig. 4. A comparison between the effective hard sphere diameters along the vapor-liquid coexistence line of Ar predicted by different models: (♦) SPT, (□) MCSL and (▲) ML, (○) Mayer-su, (●) Mayer-co, (■) PYvC, (×) CSC.

(Tables 2-4).

Figure 5 helps us to compare different approaches and have a better understanding of the variation of σ_{eff} with temperature. This figure shows that the value of σ_{eff} obtained by different methods decreases with increasing temperature with a nearly constant slope. The physical significance for temperature dependence of σ_{eff} is that at high temperatures the molecules have more energy and are capable of interpenetrating one another to a greater extent. There is also a satisfactory agreement between the values of σ_{eff} predicted by MCSL and ML models with those predicted by compressibility expressions. According to Barker [30] and Anderson [31], this phenomenon may be attributed to the fact that the present method can be treated as a simple perturbation approach. Therefore, it can be expected that the properties of reference system (HS) do not strongly affected by the perturbation factor. One may think that the values of σ_{eff} predicted by the proposed method are unrealistically small at high temperatures. This behavior may be attributed to perturbative nature of the present method, because of the fact that perturbation theories are known to systematically over-estimate the critical point and also the entire vapor-liquid

Table 2. Different Values of Effective Hard Spherical Diameters (Å) of Ar Obtained by Different Models at 6.0 MPa and Different Temperatures

	ΔH_{vap}			Compressibility		
T (K)	SPT	MCSL	ML	PY*c*	PY*v*	CS
86	3.46896	3.31426	3.31549	3.24246	3.32191	3.26489
90	3.43619	3.28153	3.28278	3.21490	3.29037	3.23641
94	3.40078	3.24638	3.24763	3.18457	3.25577	3.20506
98	3.36321	3.20930	3.21054	3.15233	3.21912	3.17176
102	3.32283	3.16967	3.17089	3.11769	3.17989	3.13597
106	3.27913	3.12697	3.12817	3.08026	3.13771	3.09732
110	3.23004	3.07926	3.08041	3.03704	3.08938	3.05275
114	3.17539	3.02639	3.02749	2.98920	3.03626	3.00347
118	3.11255	2.96588	2.96689	2.93402	2.97552	2.94675
122	3.03793	2.89429	2.89522	2.86766	2.90325	2.87870
124	2.99562	2.85383	2.85470	2.83113	2.86374	2.84130
126	2.94693	2.80734	2.80815	2.78742	2.81679	2.79664
128	2.89272	2.75566	2.75640	2.73941	2.76554	2.74766
130	2.83129	2.69721	2.69787	2.68601	2.70888	2.69328

SPT: Scaled Particle Theory, MCSL: Mansoori-Carnahan-Starling-Leland, ML: Matyushov-Ladanyi, PY*c*: Percus-Yevik (compressibility approach), PY*v*: Percus-Yevik (virial approach), CS: Carnahan-Starling. Insignificant digits are retained to avoid round-off errors.

Table 3. Different Values of Effective Hard Spherical Diameters (Å) of Xe Obtained by Different Models at 6.0 MPa and Different Temperatures

T (K)	ΔH_{vap}			Compressibility		
	SPT	MCSL	ML	PY*c*	PY*v*	CS
170	3.96753	3.78811	3.78957	3.69458	3.77775	3.71850
180	3.92299	3.74385	3.74530	3.64948	3.72613	3.67181
190	3.87038	3.69203	3.69346	3.59781	3.66750	3.61839
200	3.80753	3.63061	3.63200	3.53724	3.59943	3.55585
210	3.73028	3.55564	3.55695	3.46346	3.51748	3.47986
220	3.63233	3.46121	3.46241	3.37038	3.41543	3.38427
230	3.50381	3.33800	3.33905	3.24848	3.28375	3.25953
240	3.32613	3.16855	3.16937	3.08031	3.10509	3.08821
250	3.06037	2.91613	2.91667	2.82668	2.84067	2.83121

SPT: Scaled Particle Theory, MCSL: Mansoori-Carnahan-Starling-Leland, ML: Matyushov-Ladanyi, PY*c*:Percus-Yevik (compressibility approach), PY*v*:Percus-Yevik (virial approach), CS: Carnahan-Starling. Insignificant digits are retained to avoid round-off errors.

equilibrium curve, particularly at temperatures above about half-way between the triple-point and critical point. Although the perturbative nature of the method may be responsible for such observations, it cannot be the major reason. Such results are also obtained by compressibility approaches which are not consistent with perturbation approaches. We believe that such

Table 4. Different Values of Effective Hard Spherical Diameters (Å) of CH_4 Obtained by Different Models at 6.0 MPa and Different Temperatures

T (K)	ΔH_{vap}			Compressibility		
	SPT	MCSL	ML	PY*c*	PY*v*	CS
100	3.86234	3.69304	3.69435	3.60750	3.70190	3.63368
120	3.73722	3.56759	3.56895	3.50030	3.57871	3.52287
140	3.55794	3.39199	3.39328	3.34128	3.39935	3.35868
150	3.42912	3.26761	3.26874	3.22607	3.27208	3.24017
160	3.24662	3.09285	3.09375	3.06329	3.09584	3.07349
170	2.95121	2.81187	2.81243	2.80527	2.82329	2.81107

SPT: Scaled Particle Theory, MCSL: Mansoori-Carnahan-Starling-Leland, ML: Matyushov-Ladanyi, PY*c*: Percus-Yevik (compressibility approach), PY*v*: Percus-Yevik (virial approach), CS: Carnahan-Starling. Insignificant digits are retained to avoid round-off errors.

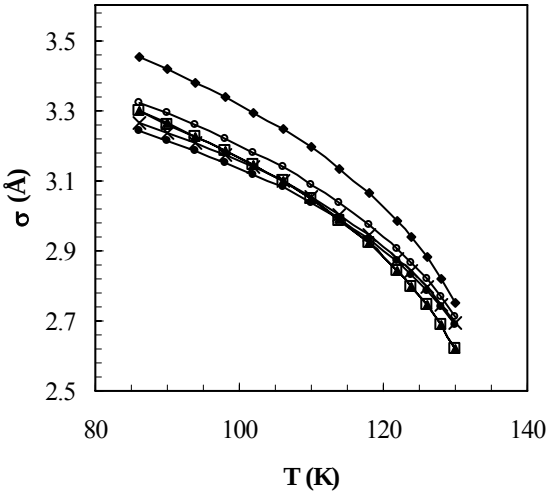

Fig. 5. A comparison between the values of effective hard spherical diameter of Ar predicted by different models at different temperature and constant pressure: (♦) SPT-H, (□) MCSL-H and (▲) ML-H, (●) PYcC, (○) PYvC, (×) CSC.

results are related to some other factors such as the rate of variation of the physical property with temperature within the interval temperature and the type of the intermolecular potential. If potential was of one parametrical type, such as those presented in Eqs. (1) and (2), all variations would be exerted on that single parameter. But when a two parametrical potential such as Lennard-Jones is being used, the variations are exerted on two parameters and consequently each parameter varies slightly with variation of temperature.

Another reason for obtaining the unrealistic small values of σ_{eff} at high temperatures is that at the $T \to T_c$ limit, the liquid behavior deviates considerably from the HS systems and is dominated by fluctuations. Therefore, in critical region, more sophisticated perturbation approaches than those presented in this work must be used.

The effect of pressure on EHSD was also investigated through Eq. (31). An arbitrary constant temperature (at which the system is in liquid state) was used in order to study this phenomenon in a wide range of pressure. The results are shown in Tables 5-7. Figure 6 is also plotted to help us to have a better understanding of the variation of σ_{eff} with pressure.

This figure shows that the value of σ_{eff} increases with increasing pressure. As previously mentioned, the expected value of EHSD is related to this fact that to what extent the given particles, which approach each other, can penetrate one another at a given temperature. Any factor which causes those particles not to penetrate considerably, will result into the bigger value of EHSD. Increasing the exerted pressure on liquid will compress the system, which in turn leads to activate the intermolecular repulsions more throughout the liquid. However, the kinetic energy is the major factor determining the extent of penetration, and increasing the pressure will compensate the effect of kinetic energy to some extent depending on the amount of applied pressure. This compensation results in a larger value of EHSD. The predicted

Table 5. Different Values of Effective Hard Spherical Diameters (Å) of Ar Obtained by Different Models at 94.0 K and Different Pressures

P/MPa	ΔH_{vap}			Compressibility		
	SPT	MCSL	ML	PY*c*	PY*v*	CS
1	3.37044	3.21647	3.21771	3.15886	3.22670	3.17854
6	3.40078	3.24638	3.24763	3.18457	3.25577	3.20506
10	3.42172	3.26711	3.26835	3.20175	3.27529	3.22281
20	3.46396	3.30916	3.31040	3.23371	3.31188	3.25584
30	3.49734	3.34266	3.34388	3.25626	3.33796	3.27918
40	3.52561	3.37122	3.37241	3.27440	3.35904	3.29796

SPT: Scaled Particle Theory, MCSL: Mansoori-Carnahan-Starling-Leland, ML: Matyushov-Ladanyi, PY*c*: Percus-Yevik (compressibility approach), PY*v*: Percus-Yevik (virial approach), CS: Carnahan-Starling. Insignificant digits are retained to avoid round-off errors.

Table 6. Different Values of Effective Hard Spherical Diameters (Å) of Xe Obtained by Different Models at 180.0 K and Different Pressures

P/MPa	ΔH_{vap}			Compressibility		
	SPT	MCSL	ML	PY*c*	PY*v*	CS
1	3.90445	3.72583	3.72728	3.65393	3.73114	3.67640
6	3.93108	3.75208	3.75353	3.67927	3.75981	3.70257
10	3.94959	3.77039	3.77184	3.69661	3.77948	3.72046
20	3.98837	3.80894	3.81039	3.73182	3.81965	3.75684
30	4.01954	3.84011	3.84154	3.75890	3.85074	3.78484
40	4.04613	3.86687	3.86829	3.78115	3.87638	3.80784

SPT: Scaled Particle Theory, MCSL: Mansoori-Carnahan-Starling-Leland, ML: Matyushov-Ladanyi, PY*c*:Percus-Yevik (compressibility approach), PY*v*:Percus-Yevik (virial approach), CS: Carnahan-Starling. Insignificant digits are retained to avoid round-off errors.

Table 7. Different Values of Effective Hard Spherical Diameters (Å) of CH_4 Obtained by Different Models at 150.0 K and Different Pressures

P/MPa	ΔH_{vap}			Compressibility		
	SPT	MCSL	ML	PY*c*	PY*v*	CS
6	3.42924	3.26773	3.26886	3.22607	3.27208	3.24017
10	3.49913	3.33501	3.33623	3.29160	3.34380	3.30742
25	3.65010	3.48157	3.48291	3.42682	3.49420	3.44668
30	3.68179	3.51261	3.51397	3.45337	3.52423	3.47410
35	3.71380	3.54403	3.54540	3.47528	3.54914	3.49676
40	3.73523	3.56514	3.56652	3.49355	3.57004	3.51566

SPT: Scaled Particle Theory, MCSL: Mansoori-Carnahan-Starling-Leland, ML: Matyushov-Ladanyi, PY*c*: Percus-Yevik (compressibility approach), PY*v*: Percus-Yevik (virial approach), CS: Carnahan-Starling. Insignificant digits are retained to avoid round-off errors.

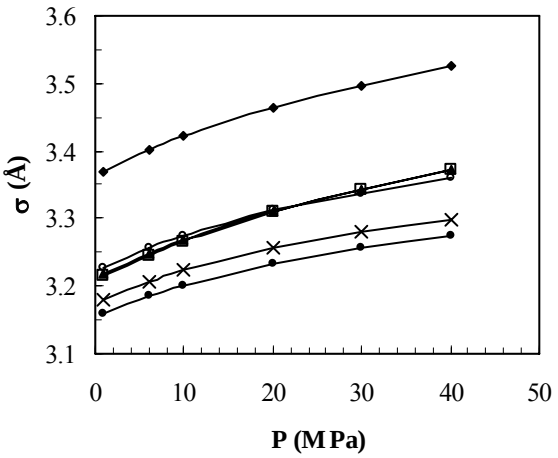

Fig. 6. A comparison between the values of effective hard spherical diameter of Ar predicted by different models at different pressure and constant temperature: (♦) SPT-H, (□) MCSL-H, (▲) ML-H, (●) PYcC, (○) PYvC and (×) CSC.

values of σ_{eff} by using SPT are again larger than those predicted by MCSL and ML models, while the slopes are the same. It should be noted that the values of $(\partial\sigma_{eff}/\partial p)_T$ which are obtained through the compressibility (Mayer's method) are smaller to some extent than those obtained using Eq. (31). We believe that this effect also originates from the fact that the compressibility expressions used by Mayer are only applicable to hard spherical fluids and if applied to real fluids some deviations in results are expected. However, based on the previous discussions, we expect that the intermolecular distances of a real system are more affected by the pressure than the intermolecular distances of a hard-sphere system.

Based on the above discussions, it can be concluded that in derivation of Eq. (22) the temperature and pressure dependency of molecular hard core diameter has to be considered, which in turn leads to:

$$\Delta\overline{H}_{vap} = RT + p\overline{V}_l + RT\eta^{cfm}_{(y)}\left[T(\alpha_p - \frac{3\sigma'_T}{\sigma}) - p(\beta_T + \frac{3\sigma'_p}{\sigma})\right] \quad (42)$$

where $\sigma'_T = (\partial\sigma/\partial T)_P$ and $\sigma'_p = (\partial\sigma/\partial p)_T$

REFERENCES

[1] R.A. Pierotti, Chem. Rev. 76 (1976) 717.

[2] G.A. Mansoori, F.B. Canfield, J. Chem. Phys. 51 (1969) 4958; Indust. Eng. Chem. (Monthly) 62 (1970) 12.

[3] H. Reiss, Adv. Chem. Phys. 9 (1965) 1.

[4] L.R. Pratt, D. Chandler, J. Chem. Phys. 67 (1977) 3683.

[5] L.E.S. Souza, D. Ben-Amotz, J. Chem. Phys. 101 (1994) 9858.

[6] D.V. Matyushov, R. Schmid, J. Chem. Phys. 105 (1996) 4729.

[7] D. Ben-Amotz, I.P. Omelyan, J. Chem. Phys. 113 (2000) 4349.

[8] H. Reiss, H.L. Frisch, J.L. Lebowitz, J. Chem. Phys. 32 (1960) 119.

[9] G.A. Mansoori, N.F. Carnahan, K.E. Starling, T.W. Leland, J. Chem. Phys. 54 (1971) 1523.

[10] B. Widom, J. Chem. Phys. 39 (1963) 2808; J. Phys. Chem. 86 (1982) 869.

[11] C. Seiter, B.J. Alder, J. Solution Chem. 7 (1978) 73.

[12] L.E.S. Souza, A. Stamatopoulou, D. Ben-Amotz, J. Chem. Phys. 100 (1994) 1456.

[13] M. Barosova, M. Malijevsky, S. Labik, W.R. Smith, Mol. Phys. 87 (1996) 423.

[14] D.V. Matyushov, B.M. Ladanyi, J. Chem. Phys. 107 (1997) 5815.

[15] M.H. Abraham, A. Nasehzadeh, J. Chem. Soc. Faraday Trans. 77 (1981) 321.

[16] A. Nasehzadeh, M. Mohseni, K. Azizi, J. Mol. Struct. (Theochem) 589-590 (2002) 329.

[17] D. Ben-Amotz, D.R. Herschbach, J. Phys. Chem. 94 (1990) 1038.

[18] A. Nasehzadeh, K. Azizi, J. Mol. Struct. (Theochem) 638 (2003) 197.

[19] D.A. Mc Quarrier, Statistical Mechanics, University Science Books, New York, 2000.

[20] A. Ben-Naim, Statistical Thermodynamics for Chemists and Biochemists, Plenum Press, New York, 1992.

[21] J.H. Hildebrand, J.M. Prausnitz, R.L. Scott, Regular and Related Solutions, Van Nostrand-Reinhold, Princeton, New Jersey, 1970.

[22] M.J. Huron, P. Claverie, J. Phys. Chem. 76 (1972) 2123.

[23] J.O. Hirschfelder, C.F. Curtiss, R.B. Bird, Molecular Theory of Gases and Liquids, John Wiley & Sons, New York, 1954.
[24] R.B. Stewart, R.T. Jacobsen, J. Phys. Chem. Ref. Data. 18 (1989) 679.
[25] O. Sifner, J. Klomfar, J. Phys. Chem. Ref. Data 23 (1994) 118.
[26] B.A. Younglove, J.F. Ely, J. Phys. Chem. Ref. Data. 16 (1987) 584.
[27] S.W. Mayer, J. Chem. Phys. 67 (1963) 2160.
[28] N.B. Vargaftik, Handbook of Physical Properties of liquids and Gases, 2nd ed., Hemisphere Pub. Co., New York, 1975.
[29] N.F. Carnahan, K.E. Starling, J. Chem. Phys. 51 (1969) 635; J. Chem. Phys. 53 (1970) 600.
[30] J.A. Barker, D. Henderson, Rev. Mod. Phys. 48 (1976) 587.
[31] H.C. Andersen, D. Chandler, J.D. Weeks, Adv. Chem. Phys. 34 (1976) 105.